

AUTONOMOUS SURFACE DEGRADATION MONITOR FOR SILICON HETEROJUNCTION SOLAR CELL

Paul McCabe¹ (pkm29)

Kehley Coleman¹ (kac196)

Neil Wang² (yxw1300)

Technical Advisor: Dr. Ina Martin, MORE Center Director of Operations, Adjunct Assistant Prof,
Materials Science and Engineering

Instructor: Professor Greg S. Lee

Submitted for EECS 399 in partial fulfillment for the degree of Bachelor of Science of
Electrical Engineering¹
Engineering Physics²

Case Western Reserve University

Spring 2022

Academic Integrity Policy

All students in this course are expected to adhere to University standards of academic integrity. Cheating, plagiarism, misrepresentation, and other forms of academic dishonesty will not be tolerated. This includes, but is not limited to, consulting with another person during an exam, turning in written work that was prepared by someone other than you, making minor modifications to the work of someone else and turning it in as your own, or engaging in misrepresentation in seeking a postponement or extension. Ignorance will not be accepted as an excuse. If you are not sure whether something you plan to submit would be considered either cheating or plagiarism, it is your responsibility to ask for clarification. For complete information, please go to <https://students.case.edu/community/conduct/aiboard/policy.html>.

The individual(s) submitting this document affirm compliance with the above statement

[This page intentionally left blank]

Executive Summary

The project aims to fine-tune the customized 4-probe TLM measuring system to achieve a user-friendly operating system with high accuracy that can directly monitor the variation in the sheet resistance of silicon heterojunction (SiHJ) solar cells upon the exposure to the accelerated aging environment. The objectives include achieving a full automation of the measuring process, a consistent result report, a straightforward data visualization, and composing a user manual for future use at the Materials for OptoElectronics Research and Education (MORE) center. The team was able to refine the TLM system to the point of <5% error in repeated measurements of contact resistance, and was able to use the newly reliable device to collect data on a cohort of SiHJ cells before and after several hundred hours of exposure. The team also completed the user manual and has identified future students who will use it to conduct further research.

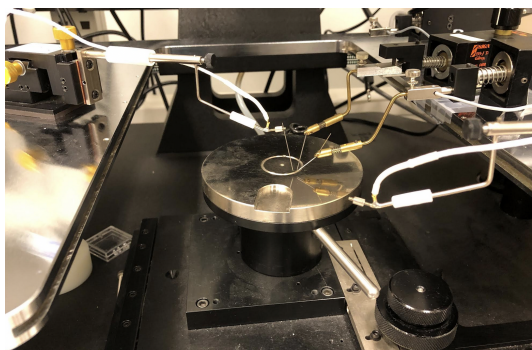
Table of Contents

Executive Summary	i
Table of Contents	ii
Problem Statement	1
Background & Context	4
Success Criteria	4
Technical Constraints	5
Standards	6
Approach & Design Methodology	7
Verification & Results	12
Project Management	16
Relevant Courses	19
References	19

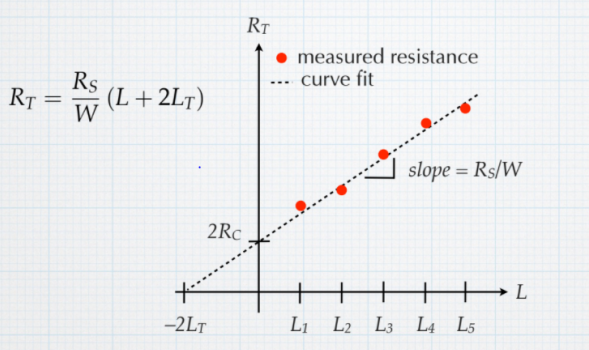
Problem Statement

Introduction of the General Problem

Frequently, researchers in centers such as the MORE Center and the Solar Durability and Lifetime Extension (SDLE) Center are interested in determining properties of solar cells such as contact and sheet resistance. One common approach used to obtain contact resistivity is TLM, or transmission line measurement. To perform a TLM measurement, one performs a four-point probe resistance measurement between two of these metal-semiconductor junctions, and then repeats the process between two junctions which are a different distance apart from each other. After acquiring resistance measurements as a function of the distance between junctions, the relationship between the two variables can be plotted; the slope of the linear plot that results is the sheet resistance of the bulk material between the metal contacts. Furthermore, the contact resistance and transfer length can be calculated from the y-intercept of the plot.



(a)



(b)

(Fig 1. TLM manual system at the University of Central Florida (a) with the resulting plot, in which the desired values like sheet resistance and contact resistivity can be extracted using linear regression (b) [1])

Often, TLM measurements are done manually, with a 4-point probe setup as shown in the Figure 1(a) above. However, there are problems with the way TLM measurements are typically performed that make them inconvenient for research here.

Problem of Manual Approach- Time

When performed manually with a 4-point probe setup, TLM is often time-consuming, inefficient, and potentially inaccurate. In order to use the 4-point probe method, the researcher must repeatedly position the probes on the narrow gridlines of a solar cell, take measurements and record data, and then move the probes to new gridlines many times on the same solar cell before the measurement is complete. This is a tedious process, and introduces a higher-than-necessary amount of human error into the measurement given that there is so much realigning that must be done in each measurement.

Problem of Commercially Available Automated Approach - Cost

There is at least one commercially available device designed to automate the TLM process and reduce the time and uncertainty that goes into each measurement: BrightSpot Automation's ContactSpot device (Figure 2)

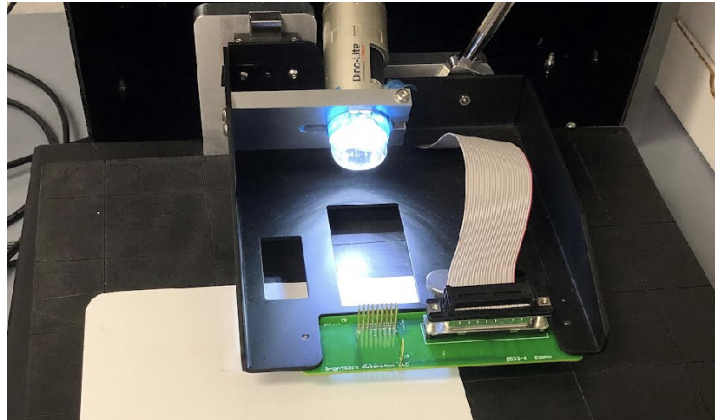


(Fig 2. BrightSpot Automation ContactSpot device courtesy of Nafis Iqbal of University of Central Florida.)

This device performs TLM measurements with fixed pins on a PCB that make contact with the solar cell at its gridlines, and automatically process the data. However, a recent quote put the device cost at approximately \$18,000. This is a very high price for this piece of equipment.

Problem for Our Design - Accuracy and Precision

In the past semester (Fall 2021) the team created a device that successfully performs TLM measurements on a solar cell using the 4-point probe method and automated measurements with a Keithley (as explained further in this report). Unfortunately both the accuracy and precision of the device did not meet pass semester's success criteria. Sheet resistance (derived from the slope) was found to be highly inconsistent while transfer length (derived from the intercept) was found to be often negative, which is theoretically impossible. Further improvements were necessary if this device is to be a viable alternative to the commercial or manual approach.

Problem of Our Design - Difficult for New Users to Learn

As mentioned previously, the past semester's work centered around making the TLM device functional. As a result, little time was allocated towards proper documentation, ease-of-use, and an instruction manual. This poses a significant problem for new researchers who wish to use the device, as without adequate documentation it is unlikely that the device will function properly.

Approach

Accuracy and Precision

The general approach for solving the inconsistent slope results from our previous device was to carefully realign the pins so that distance between the pins and level of the pins were consistent. An optical profilometer was used to discover that the grid line distance was actually 1.96mm and not the assumed 2mm, so the pins were adjusted so that each pin head sat squarely on the gridline.

The precision problem, pertaining to the negative transfer length, was diagnosed in a couple different ways. First the team measured the internal resistance of the device to determine if it played a significant role in altering the y-intercept of the graph. The initial theory was that pins farther away from the first pin

had higher internal resistance values due to their longer wires. This would theoretically alter the slope by increasing the higher pin values and decreasing the y-intercept. Experimental results indicated that this was not a significant factor.

It was noted that resistance measurements taken were inconsistent and varied with pressure of the probes using forced voltage. Forcing current on the other hand was more steady and also yielded a lower result. The second approach was to switch the TLM device to a current forcing one instead of a voltage forcing one to reduce the resistance, however this did not solve the problem either.

The third approach/theory was that the distance from the edge of the solar cell to the pins making contact was affecting results. Previous literature indicates that measured voltage increases as pins get closer to the edge of the cell. Indeed, placing pins on the very edge of the cell tended to yield positive transfer lengths; however, this was neither consistent enough nor a viable approach for research purposes. It must be something else.

Finally the team noticed the marks of the pinheads on the solar cell that were far from each grid line. It was then theorized that the path that current takes from pin to pin is significantly shorter than the values used in calculations. This is due to the outer radius of the pinhead making contact with the cell's surface, effectively reducing the distance current travels and reducing the voltage. After reducing the distance measurements by the pinhead radius $\times 2$, the effective distance current travels, all transfer lengths became positive.

Difficulty for New Users

To make the device easier to use both in setup and general measurement taking, the team set out to write a detailed user manual that lists the necessary measurement steps from start to finish. This includes necessary software packages, wiring diagrams, and troubleshooting tips. All of the technical files such as kiCad and part inventory were also listed to ensure future modifications or repairs are done seamlessly.

To improve general usability, the team also added a more detailed stage with which the cell can be placed. Outlines of the gridlines make aligning the cell easier, a raised edge assists with alignment as well, and dielectric grease on the guiding rails make raising and lowering the PCB smoother.

Benefit

The pin realignment approach successfully improved the problem of measurement precision, as making inconsistent contact with each grid line led to inconsistent slope measurements of the TLM graph.

The first three approaches to address the problem of measurement accuracy, specifically transfer length (y-intercept), did not improve the problem as they either did not fully explain the negative values or still left some of the values negative. The final approach of recalculating the true distance between pins was an improvement on the inaccurate transfer length measurements.

The user documentation and redesigning of the cell stage significantly improved the problem of ease-of-use for each measurement and the training requirements for new users. By detailing the necessary steps to set up and take measurements, the time necessary to train new users is significantly reduced. In addition, a physical guide on the stage also reduces time and effort needed to align the cell for each measurement.

Background & Context

Silicon heterojunction (SiHJ) solar cells are an advanced solar cell architecture that can help mitigate energy conversion losses typically present in traditional architectures (e.g. Al-BSF and PERC). SiHJ cells can achieve higher open-circuit voltages (V_{OC}) than is typically possible in silicon-based solar cells by eliminating contact recombination through the incorporation of amorphous silicon and transparent conductive oxide (TCO) layers into the device. However, the introduction of these TCO layers also introduces potential new pathways for degradation, which are not yet fully understood. It has been hypothesized that degradation may manifest as an increase in contact properties such as sheet resistance and contact resistivity on the cell's surface. Therefore, the ability to precisely measure these quantities over time are especially critical for characterizing the device performance and conducting research on cell degradation. This project's primary aim is to advance such research. This is why we have developed our apparatus and used it to collect data on a cohort of SiHJ cells before and after exposure to conditions designed to accelerate the degradation process.

Measuring sheet and contact resistivity of solar cells as our project focuses on, however, is just one of many techniques used to examine the degradation of cells over time. Other measurement techniques, such as crystal structure imaging and light microscopy, in addition to taking IV curve measurements and monitoring the change in cell V_{OC} and short-circuit current (I_{SC}) over time, can also be used to gather valuable information on this problem. Thus our project is part of a much larger effort to learn more about the causes and mechanisms of degradation which limits the lifetime output of solar cells. Achieving greater understanding of this solar cell degradation will help extend the lifetime of these cells, making green energy more readily accessible and inexpensive.

Success Criteria

The first success criteria for this project was to have the device set up with <10 minutes for general measurement taking by referencing the user manual (without needing to ask questions). This success criteria was met, as attaching the necessary wires and opening the correct python script takes <5 minutes with all steps outlined in the user manual. The stage with guiding lines and edges is a major contributor to this reduced time as well, since positioning the cell is normally difficult and painstaking.

The second criteria for this project was to measure values within 10% of the commercial device (ContactSpot device) using the University of Central Florida's measurements. This criteria was met successfully for sheet resistance, as the average value for UCF sheet resistance was 64.72Ohms/box and ours was 60.22Ohms/box, a 7% difference. (Same number of samples, 20) Unfortunately the counterpart of this success criteria, the transfer length, was not met as our average transfer length was found to be .021cm while UCF data was .014cm. However this is somewhat unsurprising, as the ContactSpot Transfer Length data was much more inconsistent than the sheet resistance (which we outperformed in terms of variability), indicating that measuring transfer length remains a difficult challenge for both devices. In general, though, the similarity of the performances of our device and the ContactSpot is good, and indicates the success of our device at matching the accuracy of the commercial one.

The third success criteria for this project was to record sheet resistance measurements with $<5\%$ variability for multiple measurements taken on the same solar cell at the same point in the exposure process. Meeting this precision criterion was especially important to us, as the primary goal of the research for which our device is being used is to monitor changes in cell resistance over time; thus, it is important to be able to be certain that any variance over time is due to cell degradation and not simply to

imprecision in our measurements. With a mean value of 60.22Ohms/box and a standard deviation of 2.33, this results in variability of 3.86%, which meets this success criterion. Interestingly, this SD is significantly less than ContactSpot's SD of 5.20.

The fourth and fifth success criteria that our team set had to do with conducting more research on TLM and applying our device to conduct our own research on solar cells. For our fourth criterion, our team aimed to collect and analyze data on a cohort of SiHJ cells before and after exposing them for a total of 1000 hours in a damp heat chamber that would keep them at the degrading conditions of 85 degrees Celsius and 85% humidity. For our fifth criterion, our team aimed to conduct a literature review of some existing research on TLM. While our team did not entirely meet either of these criteria as originally specified, we did make significant progress towards each. Time constraints prevented the team from being able to expose cells for a full 1000 hours (42 days), but we did collect baseline data on a set of cells, and collect more data after subjecting them to several hundred hours of exposure in the damp heat chamber. These data are analyzed in more detail in the Verification and Results section. Additionally, while our team did not complete the peer-reviewed literature review that was our deliverable for the final criterion, we did nonetheless read and prepare summaries of a variety of academic articles related to TLM, and were able to use what we learned from some of these papers to make improvements to the accuracy of our own device's transfer length measurements as outlined in the Verification and Results section.

Technical Constraints

After discussing the success criteria of our project in terms of level of automation, data accessibility, and measurement accuracy, it is time to discuss the constraints.

Resistance

To automate the process of the Keithley 2400 connecting to the pairs of pins separately and one at a time, it was necessary to introduce a variety of wires of different lengths running from different physical positions in the circuit to the D-Sub connector on our PCB. Including these wires likely also introduced additional variance in resistance. While our team tested our circuit to make sure that the effects of these varying lengths of wires were not significant enough to invalidate our measurements, they nonetheless introduce some inaccuracy that could not be entirely controlled.

Accessibility

Controlling an Arduino is usually accomplished within the Arduino IDE which performs several setup tasks. However, since one of our success criteria is to output easily accessible data, all connectivity setup and data handling needed to be done in a single Python program so that the transition from Keithley and Arduino was seamless and the user was not required to coordinate the operation of multiple programs simultaneously. This limited us to the use of the Python language in writing our program, which increased the difficulty of easily communicating with the Arduino Due to switch between pins.

Accuracy and Precision

Arguably the most difficult and vital constraint, our design needs to record measurements both accurately (as compared to the commercial device, ContactSpot) and precisely for the same solar cell to make accurate analysis over timed exposures possible. However, the individual spring constants of the pins we used do not quite match each other exactly. Thus, contact between solar cell and each individual pin might be harder to establish correctly in some places than others. In order to get an accurate measurement, we

needed to account for this by realigning some of the pin positions and applying slight pressure to the pins to ensure contact was made.

Standards

Comma Separated Values (CSV)

RFC 4180 Common Format and MIME Type for Comma-Separated Values (CSV) Files , Internet Engineering Task Force (IETF) 2005. [Online]. Available: <https://datatracker.ietf.org/doc/html/rfc4180>. [Accessed:22-Apr-2022]

Outlines and specifies the format for saving data as a Comma Separated Values (CSV) file. As indicated by the name, values (i.e. data) must be separated by commas so that the file can distinguish one data point from the next, and appropriate measures must be taken to denote line breaks (CRLF pairs) and other special characters. These guidelines are necessary for our design because they ensure that the data generated by our script is stored to the user's computer in a common format that is easy to interpret and work with for later analysis. Since our data is numerical and column names don't contain special characters, these guidelines are handled by Pandas to_csv() function.

User Interface

McMaster University - User Interface Standards - R. Jesuratnam, A. Khan, A. Mata, and J. Sandhu, Computing and Software Wiki RSS, 23-Nov-2017. [Online]. Available: http://wiki.cas.mcmaster.ca/index.php/User_Interface_Standards. [Accessed:22-Apr-2022].

Describes a standard set of user-interface guidelines to ensure a simple and intuitive process. Although our script is simple enough that it can be run from the command line even by a relatively inexperienced user and thus doesn't need a GUI, we did follow the guidelines given in this standard for error and success messages as that is what is displayed in the terminal. Examples of such guidelines for error messages include making them straightforward, easy to derive the problem area, and do not use complicated words. For success messages, our design confirms at the end of every successful measurement that it was a success by clearly displaying a summary of the data, thus indicating in real time whether a measurement was successful or whether something went wrong to give an unreasonable result.

Printed Circuit Board Files

KiCad - Schematic and PCB Layout File Formats - KiCad Web Services, 2021. [Online]. Available: <https://dev-docs.kicad.org/en/file-formats/>. [Accessed: 03-Dec-2021].

This is a combination of two standards, kicad_pcb and kicad_sch files. kicad_sch files describe the schematic of a pcb layout and compiles circuit components and connections information into a standardized file format. This file format is then translated into the actual placements of circuit

board components in the `kicad_pcb` file, which is a standard for manufacturers to print circuit boards. Our design used the KiCad application and parts libraries to assemble the schematics and PCB layout for the PCB in our device as shown below in Figure 4. Our design followed this standard because of its common use, relatively easy assembly in KiCad software, and its compatibility with manufacturer's accepted file formats.

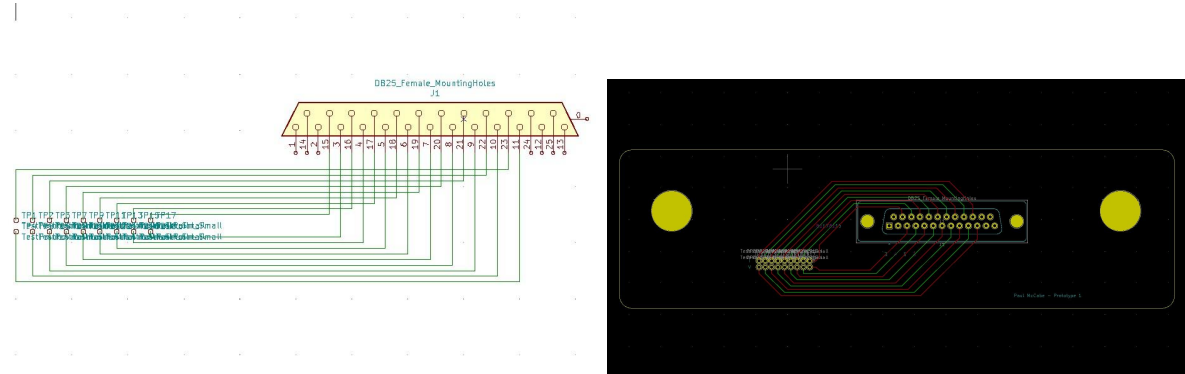


(Figure 3. schematic layout (`kicad_sch`) on the left and PCB layout (`kicad_pcb`) on the right)

Approach and Design Methodology

Pin Alignment

In order to determine why the pins were not making consistent contact with the solar cell gridlines, the team first investigated the spacing of the pins to ensure they were evenly spaced. However, measurements after this first corrective step were still inconsistent when pressed onto the solar cell. The first couple of gridlines would be in the center of the pins but gradually become more and more off-center until the last grid line would barely touch the pinhead. The team then quickly measured the distance between the gridlines to check if they were actually 2mm using a ruler.

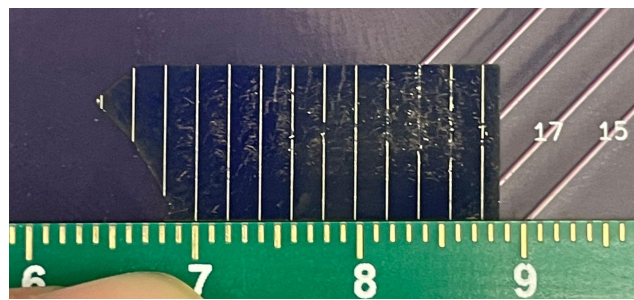


(Fig. 4, a section of degraded solar cell next to the mm measurement side of a ruler, demonstrating the <2mm distance between gridlines)

This picture shows that the grid line spacing was not 2mm, but some other fixed quantity. In order to determine this exact measurement, both for the purposes of pin alignment as well as calculation accuracy, an optical profilometer was used to measure price jumps in reflectivity on the cell as seen below.

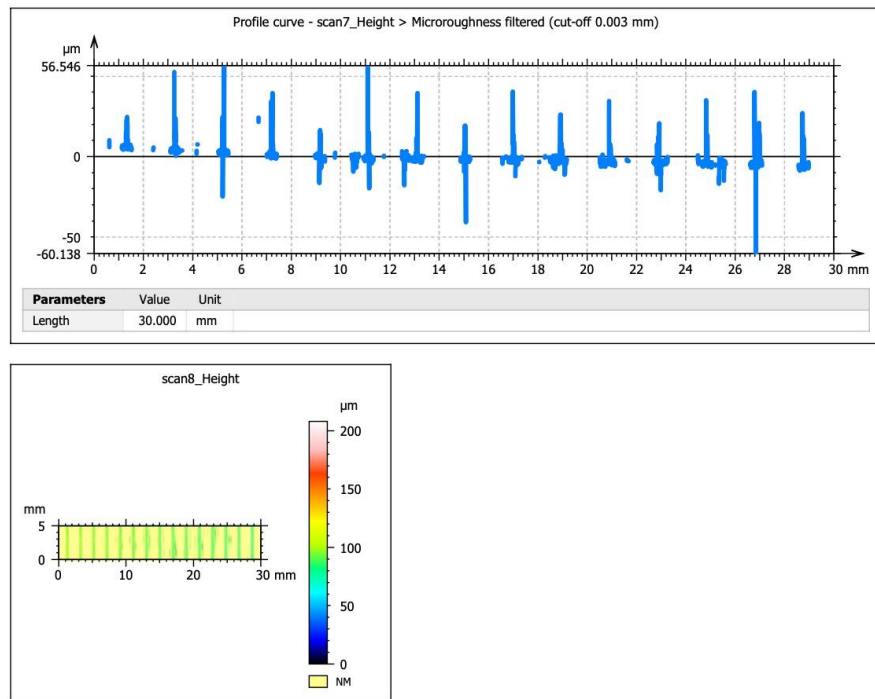


(Figure 5. Optical profilometry results which indicate the precise spacing between the grid lines)

A jump in reflectivity represents when the profilometer passes over a metal gridline, and so it was determined that the actual distance between grid lines is 1.96mm. Another realignment of the pins and correction for calculations yield consistent sheet resistance (slope) results and meets our success criteria. See the graph below which utilizes RStudio and ggplot.

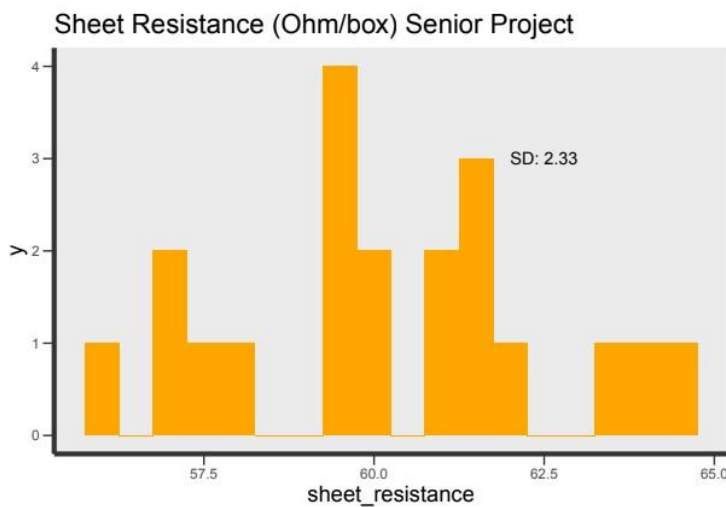


(Fig. 6, histogram of sheet resistance values using 20 measurements of a baseline sample. Graphing is done in RStudio with ggplot.)

Negative Transfer Length

The following are the 4 approaches the team utilized in order to fix the negative transfer length problem. A negative transfer length, derived from the y-intercept of the TLM graph, is theoretically impossible. Because 40% of our results had this impossible characteristic, it was vital to correct this issue before continuing to the research portion of the project.

First Approach - Internal Resistance of Device

The first approach by the team was to investigate our device for irregularities in the internal resistance. Theoretically, each pin the circuit uses different lengths of wire to transmit current from the pin, across the PCB, through the connecting wires, and so on. If the higher numbered pins (farther away) used longer wires, it could explain why the y-intercept was often negative when it should be positive. The higher numbered pins would read slightly higher resistance values than the lower numbered pins, increasing the slope slightly and decreasing the y-intercept significantly. Ultimately the circuit was designed to try and minimize this effect both with wire placement as well as the use of the 4-point probe, which minimizes the effect of internal resistance. However, 4-wire does not take into account changes in internal resistance between the current-in and current-out wires, so the team pursued this theory.

Measuring the internal resistance of the circuit using the Keithley 2400 from pin to output yielded little insight, as seen in the figure below.

Pin Type	Pin Number	Resistance Ohms forcing I	R reading forcing V
Current	1	1.05	5.27
Current	2	1.31 This one fluctuating	5.34
Current	3	0.98	4.99
Current	4	1.08 This one is fluctuating with different probe positions	5.05
Current	5	1.04	5.08
Current	6	1.38	5.1
Current	7	1.35	5.12
Current	8	1.45	5.25
Current	9	1.26	5.03
Voltage	1	0.76	5.05
Voltage	2	1.19	5.78
Voltage	3	1.67	5.38
Voltage	4	1.01	5.3
Voltage	5	0.94	5.28
Voltage	6	1.15	5.3
Voltage	7	1.1	5.27
Voltage	8	1.7	6.17
Voltage	9	0.88	5.31

(Fig. 7, all 18 pins' resistance values from the pinhead to the output wire that connects to the Keithley. Resistance measurements were taken with forcing current and forcing voltage.)

Investigating the internal resistance of the circuit did lead to an interesting phenomenon though, which is that the 2 columns (forcing I and forcing V) were different by about 4.5 ohms each time. This leads us to our second hypothesis.

Second Approach - Forcing Current over Voltage

In order to achieve the result we wanted, positive y-intercept, the team theorized that there was some missing resistance component that was artificially shifting the TLM graph downwards. (We will find later this is not the case.) One such explanation was the difference in forcing current over voltage. By adding a correction factor of approximately 4.5 volts, it could potentially shift our graph into the positive y-intercept direction. Unfortunately this approach did not work, as the measurements were originally done with forcing voltage and forcing current would actually lower our y-intercept even more.

This was a significant observation though, as the team experimented with resistors and found the forcing current measurements to be the true indication of resistance. As a result the device code was switched from forcing voltage to forcing current for more accurate measurements.

Third Approach - Varying Distance from the Sides of the Cell

Another inconsistency in the measurement taking process was the distance from the pinheads to the sides of the solar cell. Reading a paper by Siyu Guo (2017) on TLM measurements, it was discussed that distance between the pinheads and the nearby edge of the solar cell increased the measured voltage from its minimum when pins are at the center. (See below)

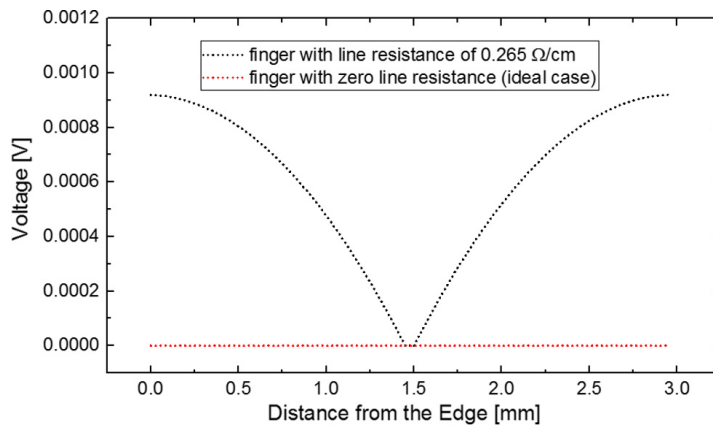


(Figure 8, the measured voltage increases near the edges of the solar cell, indicating a potential skew due to placement inconsistencies. [3])

Theoretically, this varying distance from the edge of the solar cell to the pins is caused by human positioning error and could explain why negative transfer length measurements were seemingly random. Initially the team was able to successfully determine the sign of the transfer length, making it positive when placing the pins very close to the edge and sometimes negative when placed in the middle. While it was promising to finally see a correlation between user input and the transfer length, it still did not explain why the new practice should be used over traditional practice (the ContactSpot device and manual method), nor was it consistent enough to fully explain the negative transfer length phenomenon.

Fourth Approach - Reduced Effective Current Path

One of the team members realized, when examining a degraded cell due to previous measurements, that the pinheads had left slight imprints on the solar cell substrate (blue material). This in itself was not entirely notable, as degradation due to measurements was already known and handled by applying lighter pressure. What was notable though was that these marks appeared a fair distance from the gridlines, indicating that the pins were making contact with the cell substrate at locations other than the metal gridlines. Such connections would effectively reduce each distance between pins by the radius of the first pin and the radius of the second pin, or 1mm total. Applying this correction factor using RStudio yielded positive y-intercept results for every measurement as seen below.

	sample_id	result_type	slope	intercept		sample_id	result_type	slope	intercept
0	0	normal	6049.922425	-1.773998	0	0	normal	6049.922425	4.275925
1	1	normal	6113.053918	-2.463568	1	1	normal	6113.053918	3.649486
2	2	normal	6109.713715	-1.218106	2	2	normal	6109.713715	4.891608
3	3	normal	5816.785192	1.894274	3	3	normal	5816.785192	7.711059
4	4	normal	6093.520806	-1.429982	4	4	normal	6093.520806	4.663539
5	5	normal	5727.225030	3.175097	5	5	normal	5727.225030	8.902322
6	6	normal	5800.967232	0.872880	6	6	normal	5800.967232	6.673848
7	7	normal	5892.726571	0.233725	7	7	normal	5892.726571	6.126452
8	8	normal	6058.945358	-1.583256	8	8	normal	6058.945358	4.475690
9	9	normal	6090.076187	-3.084044	9	9	normal	6090.076187	3.006032
10	10	normal	6586.311265	-4.399336	10	10	normal	6586.311265	2.186975
11	11	normal	6516.658148	-2.991855	11	11	normal	6516.658148	3.524803
12	12	normal	6335.500367	-1.347481	12	12	normal	6335.500367	4.988019
13	13	normal	6274.295554	-1.426742	13	13	normal	6274.295554	4.847553
14	14	normal	6281.987315	-1.389824	14	14	normal	6281.987315	4.892164
15	15	normal	6240.118399	-0.969088	15	15	normal	6240.118399	5.271030
16	16	normal	6253.054400	-0.737234	16	16	normal	6253.054400	5.515820
17	17	normal	6476.191731	-3.154801	17	17	normal	6476.191731	3.321391
18	18	normal	6235.852581	-0.073651	18	18	normal	6235.852581	6.162201
19	19	normal	5934.867748	2.624534	19	19	normal	5934.867748	8.559401

(Figure 9. Previous results before the correction (left) and after the correction (right) using RStudio. Notice that while every intercept increases, the slope remains constant, indicating that such a correction factor does not diminish previous accuracy found in the slope)

Design Improvements

In order to compensate for the over-extending height of the collar on the bottom of the PCB board, the team added a movable sample stage with stable support to stabilize the sample while measuring. Marks were engraved on the sample stage for an easier alignment of the grid line, as well as ensuring the measurements are tested on the same grid line. This reduces both the time required to line up a cell and take a measurement, as well as the systematic error for the final results.

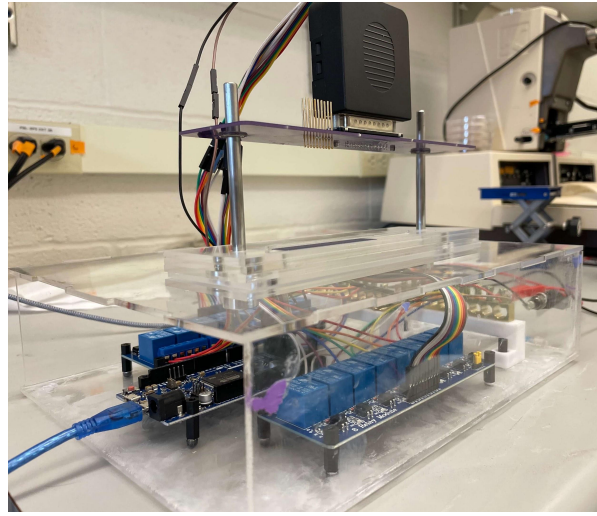


(Fig 10, Complete apparatus with sample stage, and grid line alignment marks)

Verification & Results

Repeatability of Measurements

Precision constraints for contact resistivity were set by the group as <5% error for measurements of the same sample. More specifically, this is the standard error of the mean of sheet resistance for a collection of measurements. Sheet resistance is measured as Ω/\square , or Ohms per square, and can be calculated using the contact resistivity ($m\Omega \cdot cm^2$) and the transfer length (cm) of the solar cell. Sheet resistance is derived from the slope of the resistance vs distance graph and width of the solar cell, while transfer length can be calculated with the x intercept of the same graph. As contact resistivity is the product of the contact resistance and the effective transfer area, more uncertainty is included in the calculation of contact resistivity thus introducing a greater challenge for quality measurements.

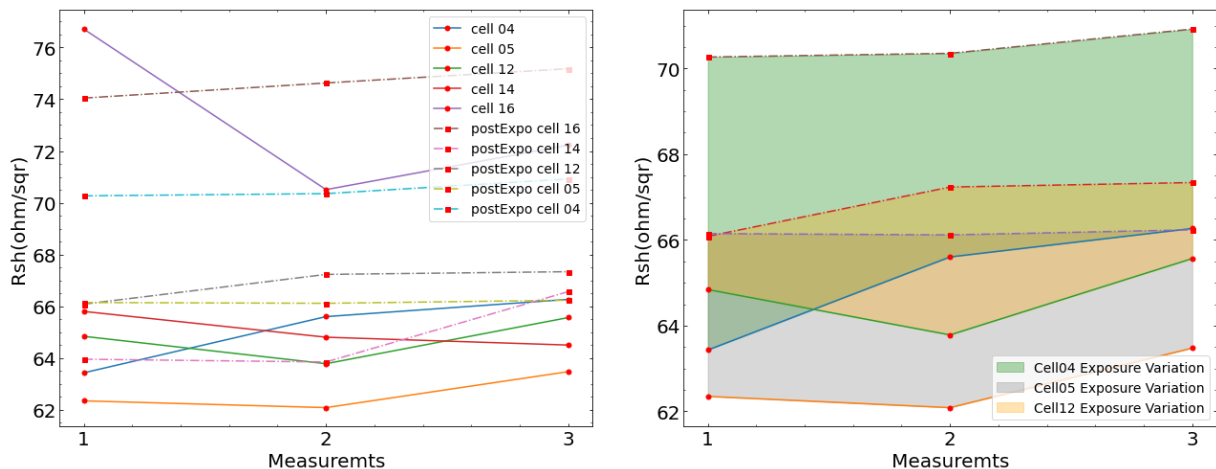


(Fig. 11, Consecutive sheet resistance results for each cell's pre and post exposure measurements. Despite a significant drop on the second measurement on cell 16, the average accuracy is 1.56%)

Results

For sheet resistance on each sample, the accuracy achieved was 1.56% as stated in Figure 11.

Measurements were obtained repeatedly on the same grid line position with similar pressure applied, and 3 measurements were consecutively taken. The repeatability of this measurement was high enough for us to confirm that our third success criterion for this project, the one about precision in our sheet resistance measurements, was met.

Voltage Sweep Results

The functionality of the measuring system is tested to be stable and clear. Each measurement can be operated under 30 seconds, depending on the number of data points that the user wants in their voltage sweep of each pair of pins. When a large number of points are sampled at each grid line, a larger range of data will be analyzed, leading to smaller deviation. The tradeoff of more points however is the increased time of operation. However, even for a relatively large sampling rate of 50 points measured between each pair of gridlines, the program will still run to completion within one minute and thirty seconds. As illustrated in Figure 11, a complete measurement was done with all the desired values shown in the graph. We then use the sheet resistance for research purposes to study the degradation impact on the HJ cell's functionality. In Figure 12, we examine the sheet resistance change after 336 hours of exposure to damp heat, where we can see there is a general increase in the resistance reading after the degradation.

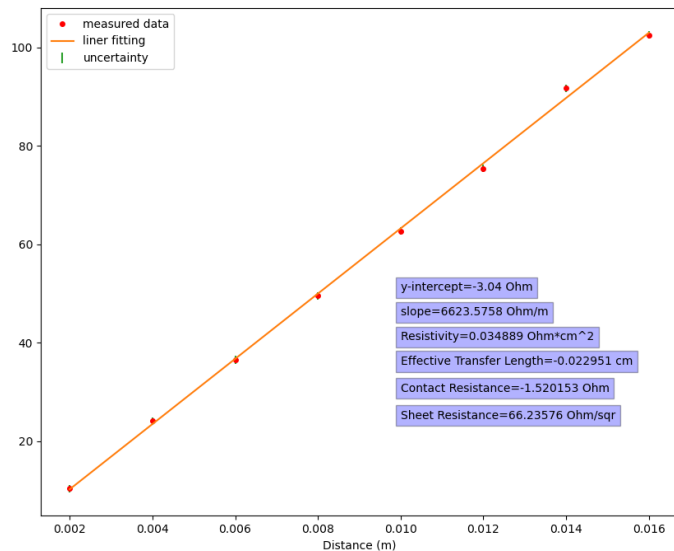


(Fig. 12, Single measurement reading for one sample with desired values like contact resistivity and sheet resistance.)

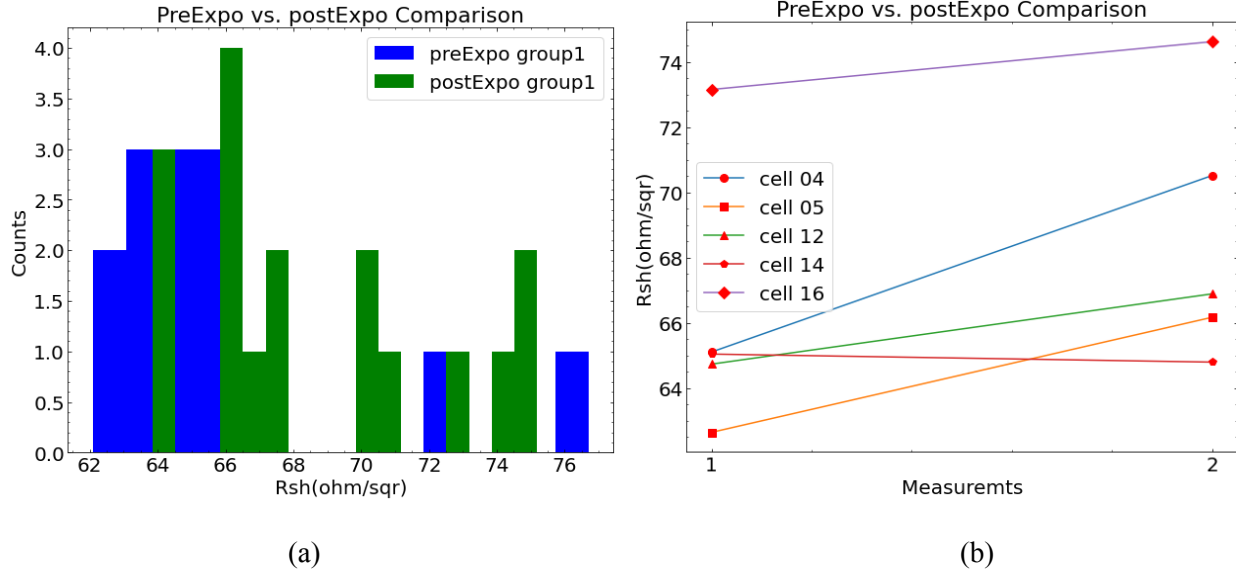


(Fig. 13, Pre-post exposure sheet resistance comparison. (a). Histogram of sheet resistance distribution of group 1 sample before and after 336 hours of damp heat. (b). Direct comparison of the sheet resistance before and after 336 hours of damp heat degradation.)

Furthermore, values along with date of measurement and sample sequential are all stored in a user-defined CSV file for further data analysis, as illustrated in Figure 13 below.

A	B	C	D	E	F	G	H	I	J	K	L	M	N	cell #
8.965424	23.0283232	38.8820036	50.800823	63.3077162	77.4576354	88.0481172	100.1084462	-1.069752881	64.96035206	-0.000164678	0.00000176	15/04/2022	12:13:18	
12.7715732	25.1769518	37.7278832	50.1971052	62.3862994	76.2548976	86.9138944	99.006536	0.292383194	61.9106958	0.0000472	0.00000138	15/04/2022	12:16:27	
13.0265506	25.4934586	38.0010018	50.4778488	62.93267	75.5968956	87.5907814	99.7420732	0.349071756	62.3105871	0.000056	0.00000196	15/04/2022	12:21:05	
10.0688482	29.6224774	43.219736	57.8478754	70.0562632	83.8556574	97.6453256	111.463848	-0.227911126	70.47591758	-0.0000323	0.000000737	15/04/2022	12:24:53	
11.8645646	25.3319862	43.0949812	57.9592386	70.2459358	84.0126588	97.940569	111.825285	-0.691618178	71.2986256	-0.000097	0.00000671	15/04/2022	12:26:54	
12.27711062	27.3840958	41.3024502	56.5665684	68.6153888	82.8095122	97.1416812	111.402256	-0.492932203	70.19249703	-0.0000702	0.00000346	15/04/2022	12:32:16	
9.01542058	23.0900538	37.7016704	52.2831542	63.3434304	75.4668124	87.8220972	99.8188058	-0.990452712	64.49967903	-0.00015359	0.00000152	15/04/2022	12:35:33	
9.02023292	25.6153522	34.1745596	52.522172	63.319802	75.2395234	87.5956476	99.7994302	-0.955697313	64.24692735	-0.000148754	0.00000142	15/04/2022	12:37:38	
9.78266476	25.6936552	40.586492	59.0575938	69.7126124	84.5052366	97.3553908	115.95774	-1.904380575	74.04453698	-0.000257194	0.0000049	15/04/2022	12:54:20	16_336hrdamp
9.75675046	25.4979348	40.4452822	58.8240944	67.0969408	85.2871208	98.0882972	116.613792	-2.231936756	74.6279445	-0.000299075	0.00000664	15/04/2022	12:56:54	16_336hrdamp_M2
9.81835118	23.5963404	40.9584486	59.4257948	67.7238778	85.2952296	98.1120632	116.83462	-2.470086414	75.17862621	-0.000328562	0.00000812	15/04/2022	12:59:11	16_336hrdamp_M3
15.2296682	28.124016	41.1784504	53.767949	67.217748	75.533301	92.0006538	104.739908	1.331555399	63.95650111	0.0000208197	0.00000277	15/04/2022	13:03:25	14_336hrdamp_M1
14.9864868	27.3168522	40.788508	54.326894	66.0323986	78.7511	91.5108448	104.3042824	1.087643613	63.85012006	0.0000170343	0.00000185	15/04/2022	13:05:28	14_336hrdamp_M2
10.88631602	24.817355	39.5719904	53.4433742	66.0062704	78.8285128	91.5692236	104.3519396	-0.613655218	66.56854442	-0.00009922	0.00000566	15/04/2022	13:08:05	14_M3
10.01514162	28.3637438	40.7830354	53.5074728	66.0068608	79.1742712	92.0304986	100.2327182	0.521906035	64.14236038	0.00008014	0.000000425	15/04/2022	13:10:13	14_M4
15.4163526	29.3337442	37.757451	54.3219952	66.9712762	84.7379338	93.8475154	105.9928074	0.796332339	66.08032199	0.0000118992	0.000000936	15/04/2022	13:13:22	12_336hrdamp_M1
11.93601076	30.822202	38.7526192	54.5484742	67.4990318	85.1896566	94.2335916	106.249792	0.322093114	67.23304022	0.0000479	0.00000154	15/04/2022	13:15:25	12_M2
11.9266493	30.8751598	38.806923	54.5571012	67.529577	85.1988774	94.3488018	106.4655006	0.304477687	67.33839606	0.000045452	0.00000138	15/04/2022	13:17:27	12_M3
10.5798432	24.1577226	36.6021676	49.6708356	62.661388	75.6287942	91.6647716	102.5343494	-1.422879902	66.14804873	0.0000215105	0.00000306	15/04/2022	13:20:37	05_M1
10.49807516	23.9925632	36.6248154	49.600727	62.5827302	75.5281646	91.5089318	102.424851	-1.454981364	66.11674551	-0.000220063	0.0000032	15/04/2022	13:22:41	05_M2
10.35046233	24.0745036	36.4756324	49.4736364	62.6709676	75.3901116	91.6659486	102.4737154	-1.520153417	66.23575827	-0.000229506	0.00000349	15/04/2022	13:24:55	05_M3
9.62716148	24.72338	38.8965004	52.2210152	69.198826	81.8837278	94.8065834	107.9320592	-1.414683593	70.26725139	-0.000201329	0.00000285	15/04/2022	13:28:17	04_M1
9.65713536	25.323409	39.1925924	56.379956	69.3256742	82.408902	95.3114958	108.1433788	-1.300166576	70.35349069	0.000184805	0.0000024	15/04/2022	13:30:26	04_M2
9.69595868	25.5329393	37.6016124	54.0813708	70.0171254	80.3279764	96.218021	108.8052818	-1.768244301	70.91906232	-0.000249333	0.00000441	15/04/2022	13:32:28	04_M3
9.52335982	23.5520732	37.4941274	51.6260994	66.8061854	80.5537396	97.2690518	110.3281334	-2.818341978	72.53406134	-0.000388554	0.0000111	15/04/2022	13:35:51	04_M4

(Fig. 14, The output data in a user-defined csv file, with detailed information provided by the computer: resistance measurements at each gridline; calculated values for sheet and contact resistance, contact resistivity, and transfer length; a date and time stamp of the time the measurement completed; the user-generated cell serial number.)

It is important to notice that while the contact resistivity varies significantly compared with the sheet resistance, the effective transfer length tends to be negative when extracted from the TLM plot due to the negative y-intercept. This indicated a problem with our measurements, as transfer length is a physical quantity that cannot be negative. Thus, our team looked into pre-existing literature on TLM to try to explain this issue and find a solution. According to Guo et al., the extracted contact resistivity from TLM is influenced by several factors: (1) strip width; (2) edge shunting; (3) current flow through unprobed grid lines; (4) non-uniform contact resistance; (5) non-uniform sheet resistance [3]. Among these potential influencing factors, the team specifically studied the effect of strip width on the extracted value.

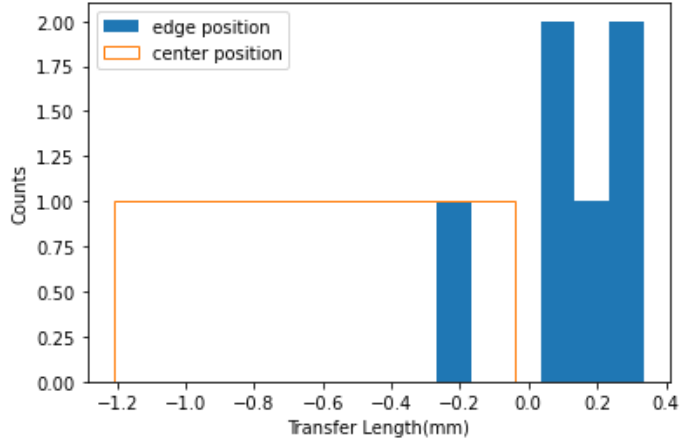


(Fig. 15, Transfer length comparison with different probe positions: probing to the center of the grid line and probing to the edge of the grid line)

In Figure 15, we can see that when measuring probes are closer to the center, the extracted effective transfer length tends to be negative whereas positive values are extracted when probing to the edge of the grid lines. Typically for HJ cells, the contact resistance doesn't vary with the increasing distance along the cell, whereas the sheet resistance changes proportionally with the distance. This can be applied to devices which either have very narrow ctrip width or highly conductive fingers. Therefore, for other cases the voltage drop along the grid line cannot be ignored. As illustrated in Figure 7, we can see a clear voltage increase moving towards the edge of the finger, and voltage diminishes to zero at the center of the line. Therefore, a higher voltage leads to a higher resistance reading when forcing a fixed current through the fingers. Eventually, this upward resistance shift would result in a seemingly positive transfer length. Another affecting factor is the electron transfer through unexpected probing contact. Due to the relatively large area of the probes, unnecessary contact will be established when placing the probes on the grid lines, thus reducing the effective grid line distances. Therefore, the distance along the x-axis will be reduced by 1 millimeter due to the 0.5mm undesired contact on each side of the grid line. After the correction on the grid line distance, a positive y-intercept can be extracted, thus obtaining a positive transfer length as illustrated in Figure 15, 16.

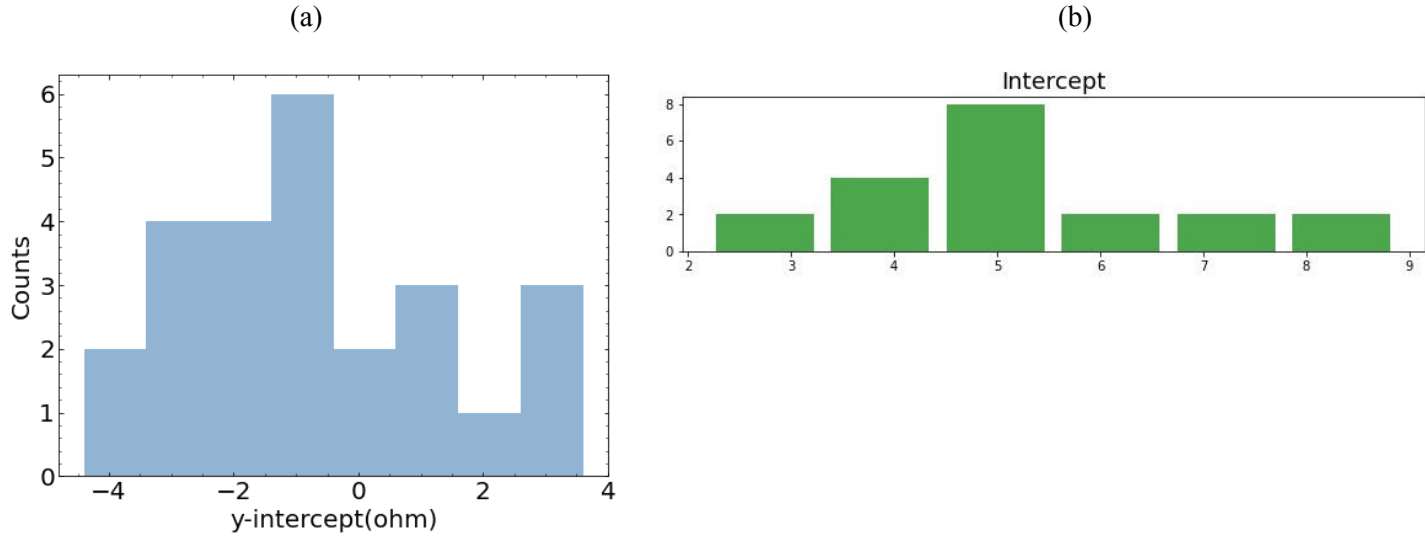


(Fig 16, Y-axis intercept comparison before and after correction of the effective grid line distance (a) Before correction the intercept converges to negative values; (b) after correction a positive shift can be seen in the intercept)

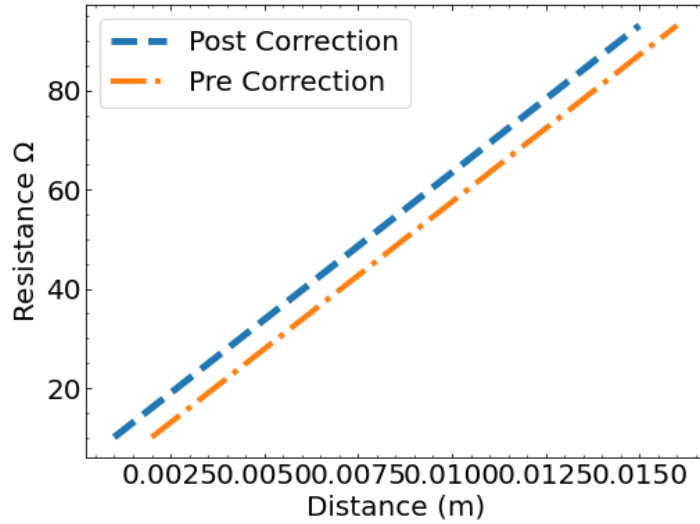


(Fig. 17, TLM total resistance vs. distance plot. A positive shift is obtained after the effective grid line distance correction, indicating positive transfer length)

Though contact resistivity and effective transfer length can be fluctuating, the sheet resistance stays consistent regardless of the correction, which is the vital element of the project. Thus, we can successfully incorporate this measuring system into further research purposes to study the surface degradation impact on the functionality of HJ cells.

Project Management

Work Breakdown

Our work breakdown structure involved essentially dividing the project into three primary subject areas: improving the accuracy and precision of our original device, make the device more generally usable, and actually using it to gather our own data. Here is a more detailed breakdown of exactly the tasks that fell under each of these three main subject areas, which we completed during the course of this project:

- Improving the accuracy of the device
 - Improving pin spacing
 - Examine cells more closely with optical profilometry to measure an actual value for gridline distance
 - Re-soldering the pins to be more horizontally level with each other and to line up better with the measured gridline distance
 - Ensure accuracy and precision are up to the required standard
 - Perform repeated measurements on the same solar cell to compare values and ensure repeatability of data
- Conduct research using the device
 - Measure a cohort of samples' baseline properties

- Expose samples to various degradation conditions
 - Measure the exposed samples once again
 - Analyze and discuss the resulting data
- Improve usability of the device
 - Write instruction manual
 - Place code in an accessible location (i.e. GitHub) and provide instructions for code installation on various operating systems so users can acquire it
 - Explain apparatus setup: wiring connections from Keithley 2400 to our TLM device and computer
 - Provide a section on troubleshooting describing how we dealt with various errors we encountered when working with our device
 - Adjust mechanical apparatus
 - Smooth the sliding mechanism of the PCB into place above the cell
 - Create a sample stage for the solar cell to assist with accurate positioning under the pins
 - Reinforce weak/flexing components in the physical design

Gantt Chart

Below is the Gantt chart our team created in OpenProject:

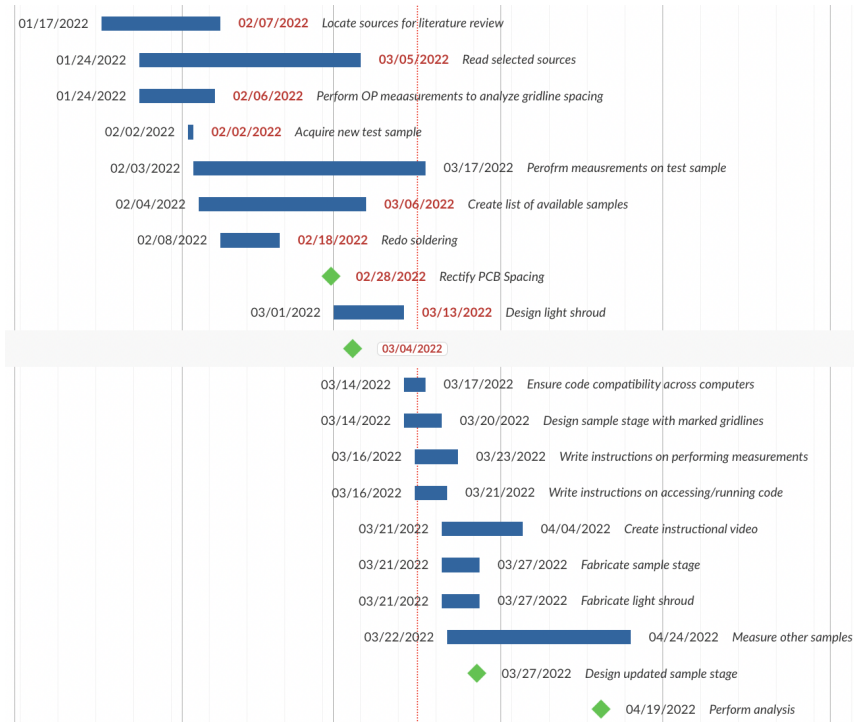


(Fig. 19, Gantt Chart)

Budget

Because this project was intended to contribute to research done by the MORE center, we received funding through our advisor (Dr. Ina Martin, operations director of the MORE center). Although we were not given a formal funding cap, we aimed to keep the cost of materials below \$500. Below is an itemized list of all of the materials we purchased in order to build our device across both semesters, with no extra costs introduced in the fine-tuning stage of the second semester. (The team was also able to utilize scrap from past purchases for the new stage)

Item	Total Cost (\$)
Spring loaded pins	74
Custom PCB	70
Arduino Due	32
Pin receptacles	32
Acrylic sheets	27
25 pin d-sub connector female	25.5
Mechanical relays	18
Shaft collars	18
25 pin d-sub connector male	13
Silicone rubber adhesive	12.50
10 pin terminal splitter	12
Color coded wires	12
Banana jack plugs	9
Flanges	4
6mm steel shafts	4
Total	363

Relevant Courses

Here are the ECSE courses taken by members of our team that proved useful to us in designing, revising, and applying our device across both semesters:

Course	Description	Role in Project
ECSE 245	Practical electronics lab work and the design of circuits containing non-linear semiconductor devices	Knowledge from this course, particularly the lab component, was applied: <ul style="list-style-type: none">● When working with the physical wiring of the circuit● When operating the Keithley 2400● When simulating performance of the original circuit design in Multisim
ECSE 321	Analysis of fundamentals of semiconductor physics, including metal-semiconductor junctions.	Knowledge from this course was applied: <ul style="list-style-type: none">● To the calculation of resistivity from the resistance measurement● To the analysis of the solar cell behavior as it pertained to the type of metal-semiconductor contact (Ohmic vs. Schottkey, etc.)
ECSE 344	The design and analysis of physical circuits, including selection of operating points for BJT & FET amplifiers and computer modeling of circuit operation.	Knowledge from this course was applied: <ul style="list-style-type: none">● In our initial drafts of our Arduino switching design, which involved using MOSFET transistors as switches

References

- [1] “TLM measurement,” *PVEducation*. [Online]. Available: <https://www.pveducation.org/pvcdrom/tlm-measurement>. [Accessed: 03-Dec-2021].
- [2] “Contact resistance,” *PVEducation*. [Online]. Available: <https://www.pveducation.org/pvcdrom/design-of-silicon-cells/contact-resistance>. [Accessed: 03-Dec-2021].
- [3] “Detailed investigation of TLM contact resistance measurements on crystalline silicon solar cells,” *University of Central Florida*. Siyu Guo 2017 [Science Direct]. Available: <https://www.sciencedirect.com/science/article/abs/pii/S0038092X1730395X>. [Accessed: 03-Dec-2021].